IEEE Access
Multidisciplinary ⋮ Rapid Review ⋮ Open Access Journal

Date of publication xxxx 00, 0000, date of current version xxxx 00, 0000.

Digital Object Identifier 10.1109/ACCESS.2017.Doi Number

Novel Ultra-Compact Quad-Channel Diplexer Using Divided Microstrip Coupled Lines for IoT, Multi-Service Wireless and 5G Networks

LEILA NOURI[1,2], FARID ZUBIR[3], SALAH I. YAHYA[4], MOHAMMED ABDEL HAFEZ[5], AND NOORLINDAWATY MD JIZAT[6]

[1] Institute of Research and Development, Duy Tan University, Da Nang 550000, Vietnam
[2] School of Engineering & Technology, Duy Tan University, Da Nang 550000, Vietnam
[3] Wireless Communication Centre, Faculty of Electrical Engineering, Universiti Teknologi Malaysia, 81310 Johor Bahru, Johor, Malaysia
[4] Department of Computer Technology Engineering, College of Technical Engineering, Al-Hadba University, Mosul 41002, Iraq
[5] Department of Electrical and Communication Engineering, United Arab Emirates University, Al Ain, United Arab Emirates
[6] Faculty of Engineering, Multimedia University, Cyberjaya, Selangor 63100, Malaysia

Corresponding authors: Farid Zubir (faridzubir@utm.my), Mohammed Abdel Hafez (mhafez@uaeu.ac.ae), and Noorlindawaty Md Jizat (noorlindawaty.jizat@mmu.edu.my)

This work was supported in part by the Higher Institution Centre of Excellence (HICOE), Ministry of Higher Education Malaysia through the Wireless Communication Centre (WCC), Universiti Teknologi Malaysia (UTM) under Grant R.J130000.7823.4J610; in part by the UTM Fundamental Research (UTMFR) under Grant Q.J130000.3823.23H92; and in part by the Faculty of Engineering, Multimedia University (MMU), Cyberjaya, Selangor, Malaysia.

ABSTRACT The rapid expansion of the Internet of Things (IoT) necessitates advanced communication technologies that can efficiently manage diverse frequency requirements and ensure reliable connectivity across various applications. This paper presents the design and analysis of a microstrip 4-channel diplexer with resonance frequencies of 700 MHz, 1.39 GHz, 2.366 GHz, and 2.9 GHz. Strategically designed to support low-power wide-area networks (LPWAN), smart device connectivity, and high-speed data transfer, this versatile diplexer addresses the critical demands of modern wireless communication systems in sectors such as smart cities, healthcare, and industrial automation. The innovative quad-band diplexer achieves remarkably Minimal insertion losses of 0.52 dB, 0.14 dB, 0.33 dB, and 0.15 dB across its four passbands, along with enhanced harmonic suppression for superior signal integrity and reduced interference. Its ultra-compact structure, measuring only $0.0028\lambda_g^2$, allows for easy integration into space-constrained environments. The use of novel, divided microstrip coupled lines significantly enhances performance while minimizing size, indicating that this diplexer can greatly improve the efficiency and reliability of wireless communication systems, paving the way for advanced multi-band operations and meeting the demands of modern multi-service and 5G networks.

INDEX TERMS Microstrip, Coupled lines, Quad-channel, Diplexer, Transfer Function, IoT.

I. INTRODUCTION

The increasing demand for efficient and compact communication systems has driven significant advancements in the design of multi-channel devices [1]. Among these, microstrip diplexers have become essential components in modern telecommunication systems, facilitating the simultaneous transmission of multiple frequency bands. However, many existing designs suffer from critical limitations that hinder their performance and applicability in real-world scenarios. For instance, several studies have highlighted common issues in traditional microstrip diplexer designs, including high insertion losses and narrow bandwidths, which significantly impact overall system efficiency [2-4]. Several types of quad-channel diplexers are proposed in [5-16], all of which are very large. In [5], a quad-channel microstrip diplexer is presented, showcasing impressive isolation metrics. However, this design is plagued by relatively high insertion losses that can severely limit its effectiveness in high-performance applications. Similarly, reference [6] proposes a multi-channel diplexer for telecommunications; however, it is characterized by narrow fractional bandwidths, which restrict its versatility across different communication scenarios. Additionally, another quad-channel diplexer introduced in [7] faces challenges with harmonic suppression and fractional bandwidth. Moreover, reference [8] explores the application of

electromagnetic simulation tools in optimizing microstrip diplexer designs; however, many existing designs fail to effectively leverage these tools, resulting in suboptimal performance predictions. Additionally, this diplexer was unable to suppress the harmonics effectively. The designed diplexer in [9] can attenuate harmonics more effectively than other references. However, its channels are very narrow, which leads to an increase in group delay. A very large matching network in reference [10] is used, which leads to a size increment. Reference [11] could improve the fractional bandwidths, but it couldn't solve the problems of large size. The theoretical analysis in reference [12] reveals trade-offs between size, bandwidth, and insertion loss that many existing designs fail to navigate effectively. In [13], there are some harmonics inside the passbands that destroy the quality of them. Also, the proposed diplexer in reference [14] was not manufactured. Despite the claim [15] about the small size, the overall size in terms of guided wavelength is not given. Meanwhile, the insertion losses in reference [16] are high. Reference [17] presents a comparative study that highlights the need for improved performance metrics; however, many designs still fall short in key areas, such as insertion loss and isolation. Finally, the case study in reference [18] presents the problems of low selectivity, large size, and undesired harmonics. The Internet of Things (IoT) is revolutionizing how devices communicate, necessitating advanced RF components that can operate efficiently across diverse frequency bands [17, 18]. According to some types of microstrip filtering devices can be used for IoT applications [19-23]. In this context, the presented microstrip 4-channel diplexer is designed to meet the growing demands of IoT applications. Fig. 1 depicts the proposed quad-band microstrip diplexer integrated with IoT Applications.

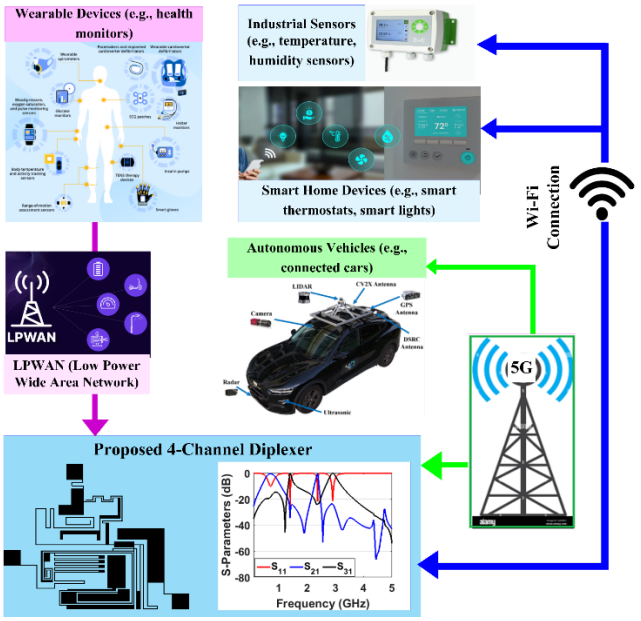

FIGURE 1. A block diagram of a quad-band microstrip diplexer integrated with IoT Applications.

In light of the other significant limitations, this paper introduces a newly designed quad-band microstrip diplexer that effectively addresses the shortcomings found in earlier works. The proposed diplexer operates across multiple resonance frequencies while showcasing significantly lower insertion losses compared to existing designs. Additionally, it achieves a broad fractional bandwidth at the first channel, enhancing its applicability in diverse communication environments. The harmonic suppression of this diplexer is notably improved, ensuring enhanced signal integrity and reducing the potential for interference. Moreover, the compact size of the proposed diplexer facilitates its integration into contemporary communication systems, where space is often a constraint. By overcoming the challenges posed by earlier designs, this diplexer represents a significant advancement in the field of multi-channel microstrip devices, paving the way for more efficient and reliable communication systems.

II. DESIGN STEPS OF THE QUAD-CHANNEL DIPLEXER

A novel basic resonator consisting of two pairs of coupled lines is exhibited in Fig. 2. Two cells are loaded on one side of one of the coupled lines. The impedance of each port (P1 and P2) will be 50Ω. The physical lengths of this basic structure are expressed by $2l_1$, $2l_2$, l_3 and l_4. In order to show how this structure can work, an approximated LC equivalent circuit of it is introduced in Fig. 2 (a).

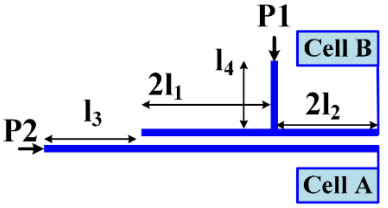

FIGURE 2. Novel proposed basic structure.

The capacitors C_A, C_B, and C_o in the equivalent LC circuit are related to the Cell A, Cell B, and open end, respectively. Each pair of coupled lines is modeled by 4 inductors and a coupling capacitor, which are highlighted in Fig. 3(a). For obtaining a more exact equivalent of coupled lines, the number of capacitors and inductors will be increased. Moreover, in this approximate circuit, we remove the effects of bends. Because the equivalents of bends and steps in widths are not effective at frequencies lower than 10GHz. The inductors L_3 and L_4 are the equivalents of thin lines with physical lengths l_3 and l_4, respectively. The open-end capacitor is very small. Consequently, we can open it. By default, the capacitors CA and CB are the equivalents of large solid microstrip cells, so that we can assume that they are short-circuited. Based on these assumptions, the LC circuit is simplified as indicated in Fig. 3(b). As highlighted in this Figure, there is a Δ connection. To simplify mathematical calculations, we used Δ to Y transformation, and the result is shown in Fig. 3 (d).

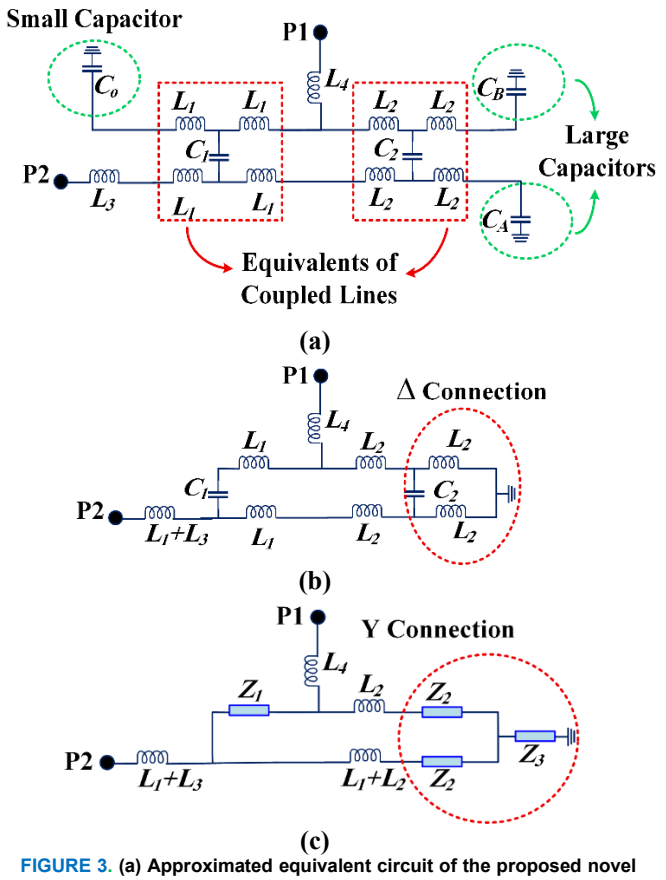

FIGURE 3. (a) Approximated equivalent circuit of the proposed novel basic structure, (b) simplified LC circuit extracted from the approximated equivalent circuit of the proposed novel basic structure, (c) Δ-Y transfer.

Analyzing the equivalent LC circuit using Fig. 3(c) is easier. Three impedances in Fig. 3(c) are calculated as follows:

$$Z_1 = j\omega L_1 + \frac{1}{j\omega C_1} = \frac{1-\omega^2 C_1 L_1}{j\omega C_1} \quad (1)$$

$$Z_2 = \frac{j\omega L_2}{1-2\omega^2 C_2 L_2} \quad (2)$$

$$Z_3 = \frac{j\omega L_2 \times j\omega L_2}{2j\omega L_2 + \frac{1}{j\omega C_2}} = -j\frac{\omega^3 {L_2}^2 C_2}{1-2\omega^2 L_2 C_2} \quad (3)$$

In equations (1)-(3), ω is an angular frequency. Simulation results show that C_1 and C_2 (coupling capacitors) are small capacitors, usually in pF or fF. The target angular frequency ω should be in GHz, and the inductor L_2 is in nH. Hence, the impedance Z_3 is very high, so we cannot open it. Consequently, the equivalent impedance between P1 and P2 will be obtained as follows:

$$Zeq = j\omega(L_1 + L_3 + L_4) + Z_4 \quad (4)$$

Where:

$$Z_4 = \frac{\left(2Z_2 + j\omega(2L_2 + L_1)\right) \times Z_1}{2Z_2 + j\omega(2L_2 + L_1) + Z_1} \quad (5)$$

If we set the impedances of ports equal to 50Ω, the transfer function of the basic structure will be calculated as follows:

$$H(j\omega) = (50 + Zeq)/50 \quad (6)$$

For Zeq(ω_r) =0, all signals can pass through the ports P1 and P2, where ω_r is an angular resonance frequency. This frequency will be obtained as follows:

$$Zeq(\omega_r) = 0 \rightarrow j\omega_r(L_1 + L_3 + L_4) + Z_4 = 0 \rightarrow$$

$$(j\omega_r(L_1 + L_3 + L_4)(2Z_2 + j\omega_r(2L_2 + L_1) + Z_1) + (2Z_2$$

$$+ j\omega_r(2L_2 + L_1)) \times Z_1)/(2Z_2 + j\omega_r(2L_2 + L_1) + Z_1)$$

$$= 0 \quad (7)$$

After calculating, equation (7) will be changed as follows:

$$j\omega_r(2Z_2L_1 + 2Z_2L_3 + 2Z_2L_4 + 2Z_1L_2 + 2Z_1L_1 + Z_1L_3 +$$

$$Z_1L_4) + 2Z_1Z_2 = {\omega_r}^2(L_1 + L_3 + L_4)(2L_2 + L_1) \quad (8)$$

Substituting equations (1) and (2) in (8) results:

$$\frac{2L_1 + 2L_2 + L_3 + L_4}{C_1} =$$

$$2{\omega_r}^2\frac{L_1L_2 + L_3L_2 + L_4L_2}{1 - 2{\omega_r}^2C_2L_2} - 2\frac{1 - \omega r^2 C_1L_1}{1 - 2\omega r^2 C_2L_2}\frac{L2}{C1}$$

$$+{\omega_r}^2(4L_1L_2 + 3L_1L_2 + 2L_3L_2 + 2L_3L_1 + 2{L}^2L_4 + 2L_4L_1) \quad (9)$$

If the thickness of lines, and also the space of coupled lines, are equal, with a good approximation, coupling capacitors are close to each other ($C=C_1\approx C_2$). Therefore:

$$(1 - {\omega_r}^2C_1L_1)/(1 - 2{\omega_r}^2C_2L_2) \approx 1 \quad (10)$$

Moreover, because of having small coupling capacitors, it can be approximated that:

$$\frac{L_1L_2 + L_3L_2 + L_4L_2}{1 - 2\omega r^2 C_2L_2} \approx 0 \quad (11)$$

Now equation (9) is reduced as follows:

$$\omega_r \approx \sqrt{\frac{2L_1 + 4L_2 + L_3 + L_4}{(4L_1L_2 + 3L_1^2 + 2L_3L_2 + 2L_3L_1 + 2L_2L_4 + 2L_4L_1)C}} \quad (12)$$

According to the last equation, by setting C and the inductors in fF and nH, we will reach the target range of resonance frequency. For a predetermined target resonance frequency, the values of inductors and coupling capacitors will be tuned. Only Cells A and B should be large enough. Using the proposed basic structure, a novel resonator is proposed and depicted in Fig. 4(a). This resonator does not consist of cells A and B (shown in Fig. 2). Therefore, its frequency response will not be perfect. Fig. 4(b) illustrates the frequency response of the proposed resonator. The dimensions of P1 and P2 terminals are tuned for connecting to 50 Ω connectors. These dimensions are obtained based on using a substrate of Rogers_RT_Duroid5880 (ε_r=2.2, h=0.7874mm, and tan(δ)=0.0009). This substrate is used for simulating all layouts in this work. The simulation results are extracted by ADS software (EM simulator with small linear steps). This resonator should be upgraded to improve the frequency response.

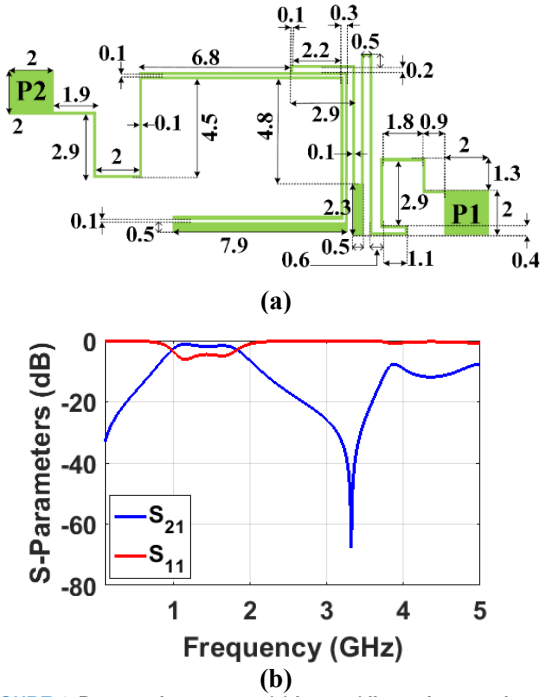

FIGURE 4. Proposed resonator: (a) layout (dimensions are in mm and the widths of all thinnest lines are 0.1mm), (b) frequency response.

A compact meandrous cell is added to the proposed resonator as shown in Fig. 5(a). The other dimensions are exactly equal to the proposed resonator in Fig.4(a). Since we need a dual-band bandpass filter, we have to create another passband. This additional cell helps to create the second channel. The frequency response of this resonator is presented in Fig. 5(b). It can be seen that the meandrous cell can help to create the 2nd channel, but it's not enough.

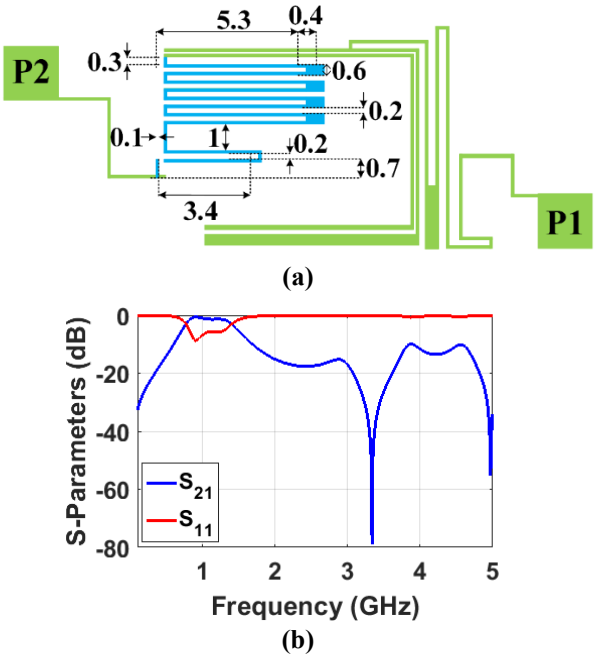

FIGURE 5. Adding a meandrous cell to the proposed resonator: (a) layout (dimensions are in mm and the widths of all thinnest lines are 0.1mm), (b) frequency response.

Accordingly, a solid large cell is added to the proposed resonator (as shown in Fig. 5(a)) and is depicted in Fig. 6(a). The frequency response of the proposed layout configuration in Fig. 6(a) is exhibited in Fig. 6(b).

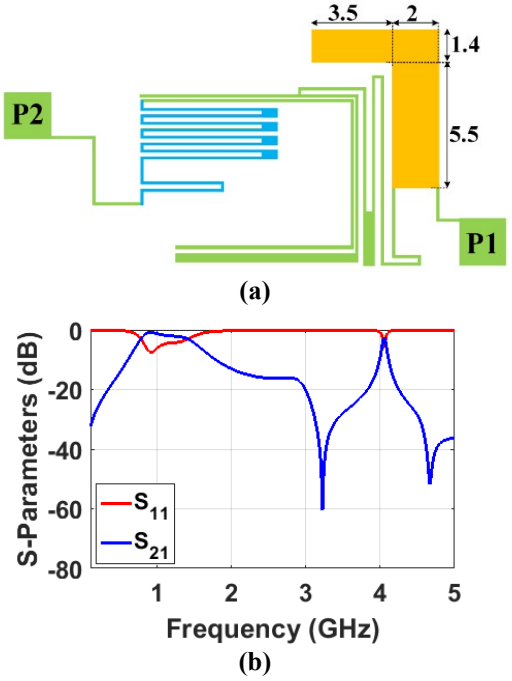

FIGURE 6. Adding a solid large cell to the proposed resonator: (a) layout (dimensions are in mm), (b) frequency response.

It can be seen in Fig. 6(b) that the second channel can be obtained at this level. But the quality of this channel is weak yet. Also, the selectivity of the 1st channel is poor. To increase the selectivity of the lower channel, we increased the length of coupled lines by adding a pair of spiral coupled lines. Under this condition, the proposed layout is changed as indicated in Fig. 7(a). In this case the frequency response is revealed in Fig. 7(b). adding these spiral coupled lines could improve the frequency selectivity of the first passband. However, to improve both channels we have to add two large solid cells (as mentioned in the mathematical analyze).

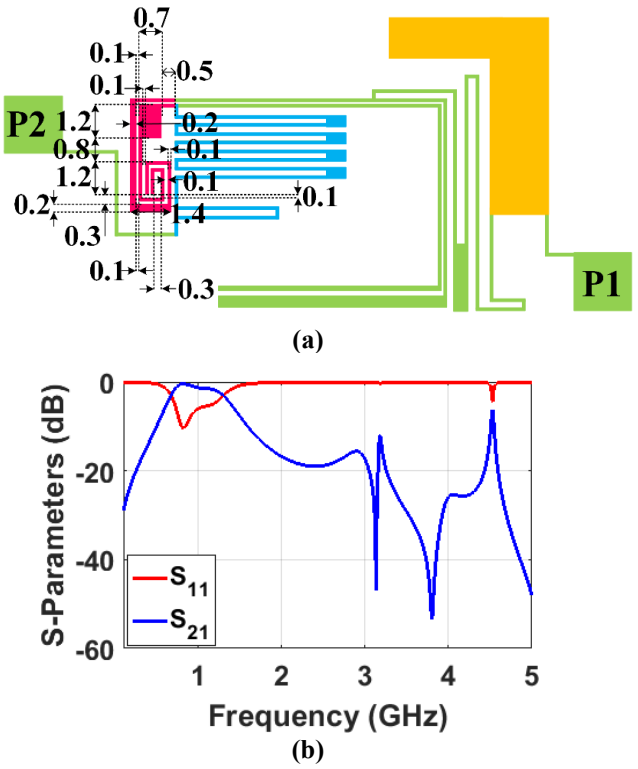

FIGURE 7. Adding a pair of spiral coupled lines to the proposed resonator: (a) layout (dimensions are in mm and the widths of all thinnest lines are 0.1mm), (b) frequency response.

The proposed novel dual-band bandpass filter is obtained as its layout and frequency response are clarified in Figs. 8(a) and 8(b) respectively. The layout configuration of the dual-band filter is very compact. All cells are embedded inside the main body of the proposed resonator to save the size. As displayed in Fig. 8(b), the proposed filter can suppress the harmonics to 4GHz. The frequency selectivity is improved for both channels and the losses are acceptable. In this step we can add the third port named as P3.

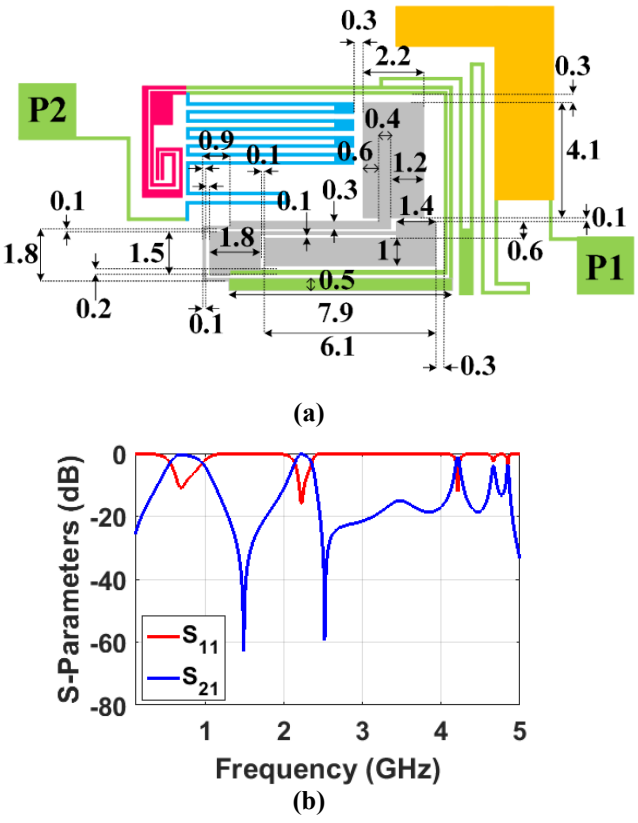

FIGURE 8. Dual-band bandpass filter: (a) layout (dimensions are in mm and the widths of all thinnest lines are 0.1mm), (b) frequency response.

Fig. 9(a) demonstrates a geometrical structure which is obtained by adding a pair of coupled lines and P3 to the designed dual-band bandpass filter. In this structure, enough space for adding other cells is predicted. Also, the coupled lines are well structured for saving the overall size. Fig. 9(b) depicts the frequency response of the primary 3-port network. As shown 3 channels are appeared a channel is suppressed due to its location. This channel is stuck between channels 2nd and 4th. Also, the quality of two new channels is not well.

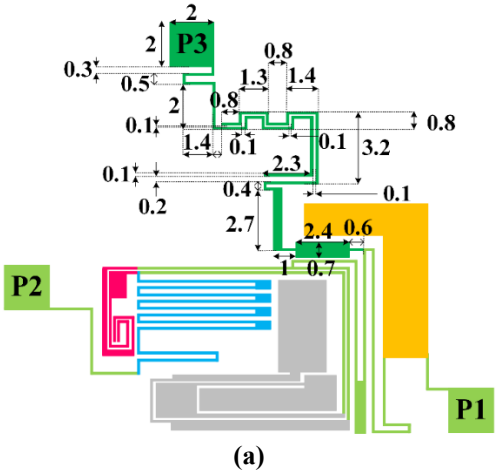

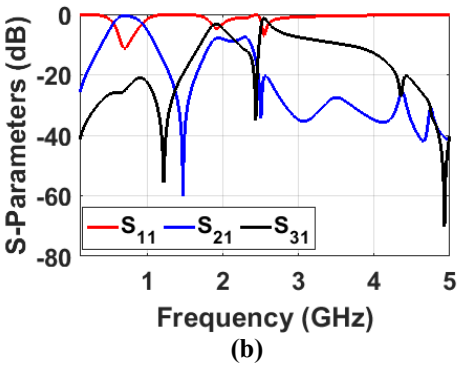

FIGURE 9. (a) Layout of the primary 3-port microstrip structure (dimensions are in mm), (b) the frequency response of primary 3-port microstrip structure.

To increase the quality of two new channels two cells are added as presented in Fig. 10 (a). These cells have capacitance feature as expected from analyzing the basic structure. The scattering parameters of this structure are shown in Fig. 10 (b). As demonstrated, the bandwidths of two new channels are better than previous state. But the third channel has not yet appeared. To solve this problem a long thin meandrous cell is added to achieve the final quad-band diplexer. The final geometrical structure of the proposed quad-band diplexer is manifested in Fig. 11, where all dimensions are in mm. The not shown sizes are the same as previous images and have not changed.

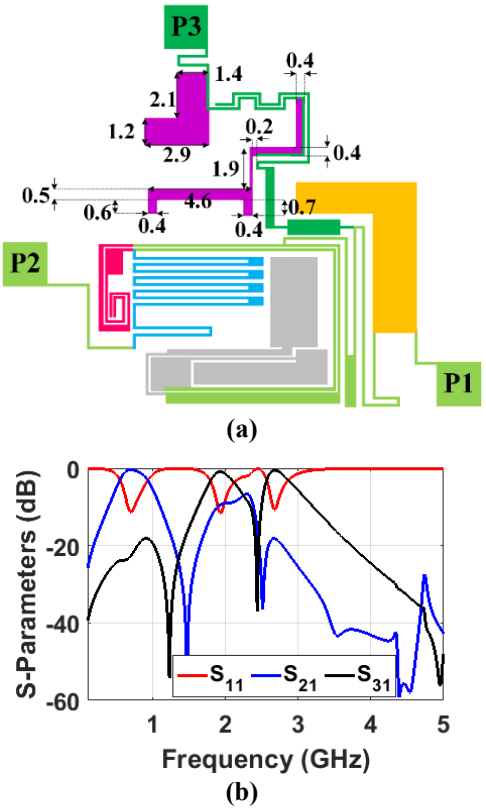

FIGURE 10. (a) Adding two cells in the layout of the 3-port microstrip structure (dimensions are in mm), (b) the frequency response of Fig. 9(a).

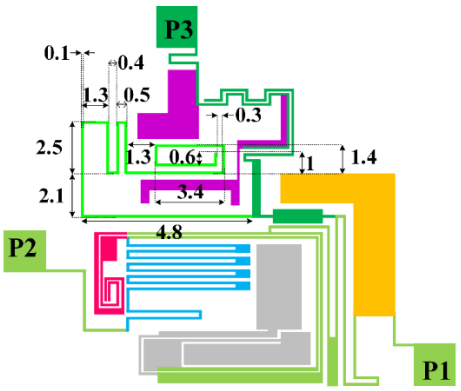

FIGURE 11. Geometrical layout of the designed quad-band diplexer (all dimensions are in mm).

III. RESULTS AND DISCUSSION

The scattering parameters, both simulated and measured, for the designed quad-band diplexer are illustrated in Figs. 12 (a), (b) and (c). As shown in Fig. 12 (a) and (b), the diplexer exhibits four distinct passbands corresponding to resonance frequencies of 700 MHz (from 548 to 873 MHz), 1.397 GHz (from 1.365 to 1.441 GHz), 2.366 GHz (from 2.3 to 2.388 GHz), and 2.902 GHz (from 2.789 to 3.014 GHz). The simulated insertion losses at these resonance frequencies are recorded as 0.52 dB for the first band, 0.14 dB for the second, 0.33 dB for the third, and 0.15 dB for the fourth. These values indicate efficient signal transmission across the specified frequency ranges. In addition, Fig. 12 (c) presents a close-up view of the return loss at the common port for the first through fourth channels, which measures 10.2 dB, 25.6 dB, 21.8 dB, and 21.3 dB, respectively. These return loss values signify good impedance matching and reflectivity, essential for optimal performance in communication systems. The isolation between channels is notably greater than -19.19 dB, which is advantageous for minimizing interference between the channels and ensuring signal integrity. Moreover, the harmonics are suppressed up to 5 GHz which verify that from 1st to 6th harmonics are attenuated. It is important to note that the simulated losses are slightly more favorable than the measured results due to inherent connector and copper losses. The measurements were conducted using a ZNB40 vector network analyzer, ensuring accuracy in the assessment of the diplexer's performance. The overall dimensions of the proposed diplexer are 16.3 mm × 17.7 mm, which corresponds to $0.051\lambda_g \times 0.055\lambda_g$, where λ_g is calculated at the first resonance frequency of the diplexer. The design of this quad-band diplexer not only demonstrates effective frequency separation but also highlights its potential applications in modern communication systems, particularly in scenarios requiring multi-band operation. The performance metrics achieved indicate that this diplexer can be a valuable component in enhancing the efficiency and reliability of wireless communication networks. For verifying the advantages of this multi-channel diplexer, we compared it

with the other microstrip diplexers. The comparison results are expressed in Table1, where the parameters F, IL, and HS are the resonance frequency, insertion loss and harmonic suppression respectively. Also, the indexes 1, 2, 3 and 4 are related to the 1st, 2nd, 3rd and 4th channel respectively.

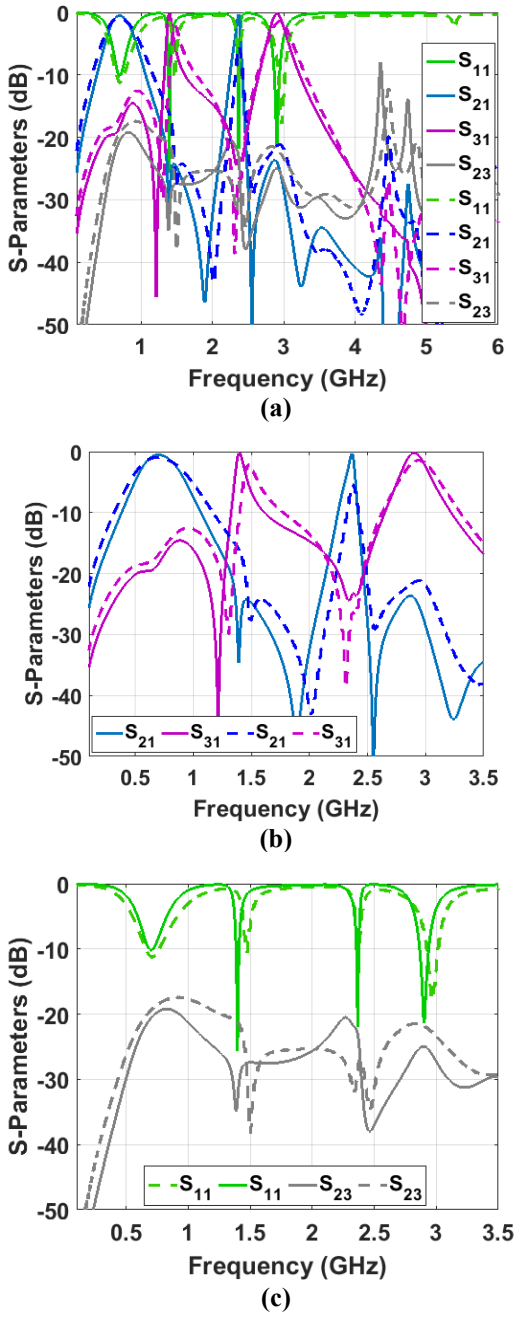

FIGURE 12. Simulated and measured: (a) wide-band view S_{11}, S_{21}, S_{31}, S_{23}, (b) close up view of S_{21} and S_{31}, (b) close up view of S_{11} and S_{23} (Dotted: Measurements & Solid: Simulations).

TABLE I. COMPARISON OF THIS DIPLEXER WITH THE OTHER QUAD-CHANNEL DIPLEXERS.

Refs.	F_1, F_2, F_3, F_4 (GHz)	Fractional Bandwidths	Size (λg^2)
	IL_1, IL_2, IL_3, IL_4 (dB)	HS	
This	0.7, 1.39, 2.36, 2.9	47%, 5.4%, 3.7%, 7.7%	0.0028
	0.52, 0.14, 0.33, 0.15	7.14 F_1	
[5]	2.14, 2.4, 3.8, 4.5	6.5%, 6%, 4%, 4.3%,	---
	2.10, 2.82, 1.95, 2.6	2.5 F_1	
[6]	1.68, 1.9, 3.9, 4.43	Very Narrow	0.051
	0.68, 0.57, 0.71, 0.5	3.7 F_1	
[7]	1.7, 1.9, 3.3, 3.6	Very Narrow	0.0233
	0.53, 0.55, 0.78, 0.87	3.5 F_1	
[8]	1.85, 2.45, 2.1, 3.5	5.4%, 4%, 4.6%, 5.7%	0.07
	1.7, 1.2, 2.3, 0.65	2.7 F_1	
[9]	1.67, 2.5, 3.4, 4.5	Very Narrow	0.029
	0.5, 0.38, 0.53, 0.58	4.8 F_1	
[10]	0.9, 1.2, 1.5, 1.8	7.2%, 5%, 7.3%, 4.1%	0.049
	1.36,1.5, 1.3, 1.6	3.05 F_1	
[11]	2.45, 3.5, 4.2, 5.2	12.5%, 7.2%, 6.4%, 5%	0.897
	0.22, 0.3, 1.3, 2.12	2.45 F_1	
[12]	2.07,2.3, 3.9, 4.49	Very Narrow	0.025
	0.59, 0.41,0.45, 0.73	3.6 F_1	
[13]	1.65, 2.5, 4.65, 6.9	Undesired channels	---
	---	4.2 F_1	
[14]	1.08, 1.17, 2, 2.18	13.8%, 15.2%, 9%, 6.1%	---
	1.18, 1.24, 1.24, 1.37	4.6 F_1	
[15]	2.15, 2.7, 3.6, 5.05	8.1%, 5.8%, 3.06%, 4.3%	0.0926
	0.81, 1.43, 1.32, 0.9	2.5 F_1	
[16]	3.5, 4, 5.7, 6.3	5.2%, 5%, 6.2%, 5.3%	0.01
	0.8, 0.8, 0.5, 0.9	2F_1	

The proposed diplexer stands out with resonance frequencies of 0.7 GHz, 1.39 GHz, 2.36 GHz, and 2.9 GHz, which are strategically positioned to cater to a wide range of communication applications. The insertion losses at these frequencies are remarkably low. These values indicate efficient signal transmission, particularly when compared to other diplexers in the table, which generally exhibit higher insertion losses. For instance, the diplexer referenced in [5] has insertion losses ranging up to 2.82 dB, significantly higher than those of the proposed design. Moreover, the fractional bandwidths of the proposed diplexer are noteworthy. It achieves a fractional bandwidth of 47% at the first channel, which is substantially higher than many of the alternatives listed, such as those from references [6] and [7], where the bandwidths are categorized as "Very Narrow." This broad bandwidth allows for more flexible and efficient channel utilization, making the diplexer suitable for applications requiring robust performance across varying bandwidths. In terms of harmonic suppression, the diplexer demonstrates a harmonic suppression level of 7.14 at the first resonance frequency (F_1), which is competitive when compared to other designs. For example, the diplexer from reference [6] achieves a harmonic suppression of 3.7 at F_1, indicating that the proposed diplexer may provide better performance in minimizing unwanted harmonic signals, thus enhancing overall signal integrity. Finally, the compact size of the proposed diplexer, measuring only 0.0028 λ_g^2, further emphasizes its advantages. This small footprint is advantageous for integration into modern communication systems where space is at a premium. In contrast, several

other diplexers in the table have larger sizes, which could be limiting in certain applications. Finally, two photographs of the manufactured quad-channel diplexer are depicted in Fig. 13.

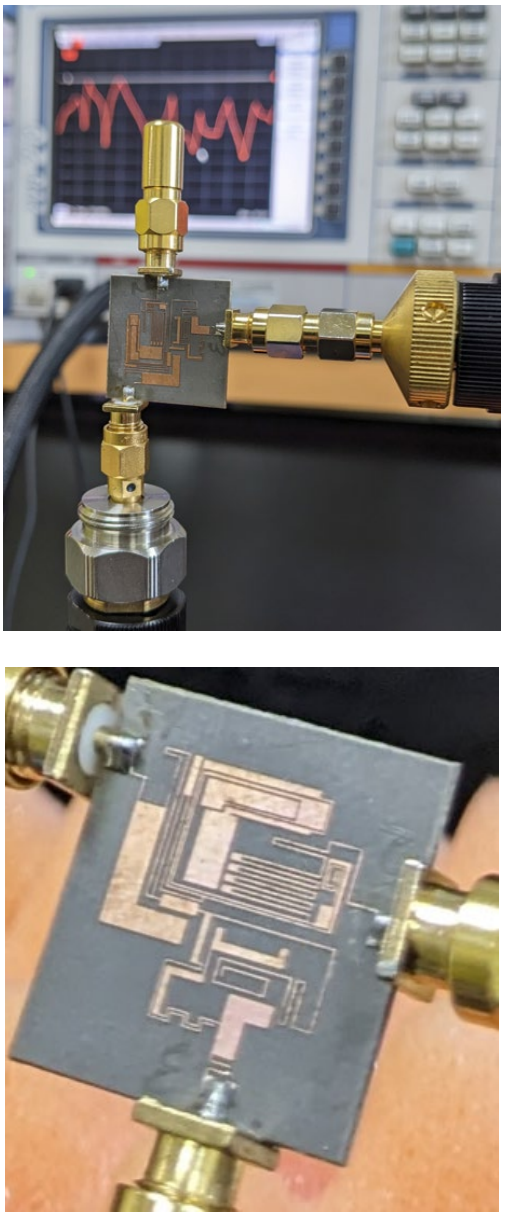

FIGURE 13. **Photos of fabricated diplexer.**

IV. APPROPRIATENESS OF THE MICROSTRIP 4-CHANNEL DIPLEXER FOR IOT APPLICATIONS

The microstrip 4-channel diplexer designed with resonance frequencies of 700 MHz, 1.39 GHz, 2.36 GHz, and 2.9 GHz, along with fractional bandwidths (FBWs) of 47%, 5.4%, 3.7%, and 7.7%, respectively, presents a compelling case for its application in the Internet of Things (IoT) landscape. The following discussion outlines the reasons this diplexer can be deemed appropriate for IoT applications.

Justification for IoT Suitability:

1-Diverse Frequency Spectrum:
700 MHz Band: This frequency is particularly valuable for low-power wide-area networks (LPWAN), which are essential for long-range communication in IoT applications. It supports devices that require minimal power consumption while maintaining reliable connectivity over large distances. Use cases include smart agriculture, remote environmental monitoring, and utility metering.
1.39 GHz Band: This frequency is commonly associated with various wireless communication standards.
2.36 GHz Band: With an FBW of 3.7%, this frequency supports emerging technologies, including aspects of 5G, allowing for high-speed data transfer and enhanced connectivity for smart devices and applications.
2.9 GHz Band: This frequency, with an FBW of 7.7%, is well-suited for high-speed data transfer and short-range applications. It is ideal for scenarios such as video streaming, augmented reality, and connected home devices, where high data rates are essential for functionality.

2-Fractional Bandwidths (FBWs):
700 MHz Band: FBW of 47% is appropriate for LPWAN applications.
1.39 GHz Band: FBW of 5.4% is noted, and this frequency is often used for various wireless communication standards, though not specifically for 5G.
2.36 GHz Band: FBW of 3.7% is suitable for supporting aspects of 5G technologies.
2.9 GHz Band: FBW of 7.7% is well-suited for high-speed data applications, including video streaming.

3-Diverse Frequency Spectrum:
The explanation of how each frequency band supports different IoT applications aligns with common uses in the industry, such as:
700 MHz for long-range, low-power applications (LPWAN).
1.39 GHz for general smart device connectivity.
2.36 GHz for emerging 5G technologies.
2.9 GHz for high-speed, short-range applications.

4-Multi-Channel Functionality:
The diplexer's ability to operate across multiple channels allows for simultaneous communication, which is vital in IoT environments where multiple devices need to transmit and receive data concurrently. This feature enhances the overall efficiency of the network, reducing latency and improving user experience.

5-Energy Efficiency:
The low insertion losses across the diplexer's frequency bands ensure that power consumption is minimized, which is crucial for battery-operated IoT devices. This efficiency

aligns with the growing demand for sustainable and energy-conscious technologies in the IoT sector.

6-Compact Design:
The compact nature of the diplexer makes it suitable for integration in space-constrained environments, such as wearable devices, smart sensors, and embedded systems. This adaptability is crucial as IoT devices continue to shrink in size while increasing in functionality.

7-Support for Emerging Technologies:
The inclusion of bands that align with future wireless standards, particularly in the higher frequency ranges, positions this diplexer as a forward-looking solution that can accommodate the evolving requirements of IoT applications.

Finally, the microstrip 4-channel diplexer is well-suited for IoT applications due to its diverse operating frequencies, robust multi-channel capabilities, energy efficiency, and compact design. Its ability to support both long-range and high-speed communication makes it a versatile component in the rapidly expanding IoT ecosystem, enabling applications across various sectors such as smart cities, healthcare, and industrial automation. This diplexer represents a significant advancement in enhancing connectivity and performance in modern wireless communication systems.

V. CONCLUSION

The proposed quad-band microstrip diplexer represents a substantial advancement in the field of multi-channel devices, effectively overcoming the limitations of earlier designs. Meanwhile, it is suitable for the Internet of Things. By achieving low insertion losses, broad fractional bandwidths, and improved harmonic suppression, this diplexer enhances signal integrity and minimizes interference, making it suitable for a wide range of communication applications. This structure is analyzed mathematically to find the novel basic structure behavior and easy optimization. The innovative design, characterized by its compact size, positions it as a valuable component in modern communication systems where space and performance are critical. The results from simulations and measurements confirm the diplexer's exceptional performance. Future work will focus on further optimizing the design and exploring its applications in emerging communication technologies, ensuring that it meets the evolving demands of the industry.

REFERENCES

[1] S. Roshani, S.I Yahya, Y.Y Ghadi, S. Roshani, F. Parandin, B.D. Yaghouti, “Size reduction and harmonics suppression in microwave power dividers: A comprehensive review”, Aro-the scientific journal of koya university, vol. 11, no. 2, pp. 122-136, 2023.

[2] S.I. Yahya, F. Zubir, M.A. Hafez, L. Nouri, M.A. Chaudhary, M. Assaad, A. Rezaei, N.M. Jizat, “Novel high-performance microstrip diplexer for 5G mid-band and wide-band applications: Design, analysis and manufacturing”, PLoS One, vol. 20, no. 7, pp. e0327839, 2025.

[3] L. Johnson, M. Lee, “A novel dual-band microstrip diplexer with enhanced filtering mechanisms”, Journal of Electromagnetic Waves and Applications, vol. 36, no. 7, pp. 987-999, 2022.

[4] R. Chen, H. Wang, “Experimental investigation of substrate materials on microstrip diplexer performance”, Microwave and Optical Technology Letters, vol. 65, no. 2, pp. 456-461, 2023.

[5] A.K. Gorur, A. Turkeli, M. Buyuktuna, E. Dogan, C. Karpuz, A. Gorur, “A high isolation quad-channel microstrip diplexer based on codirectional split ring resonators”, Microw Opt Technol Lett., vol. 64, pp.1382–1386, 2022.

[6] A. Rezaei, L. Noori, M.H. Jamaluddin, “ Design of a novel microstrip four-channel diplexer for multi-channel telecommunication systems”, Telecommunication Systems, vol. 72, pp. 189–197, 2019.

[7] S. Roshani, S.I. Yahya, Y.S. Mezaal, M.A. Chaudhary, A.A. Al-Hilali, A. Mojirleilani and S. Roshani, “Design of a Compact Quad-Channel Microstrip Diplexer for L and S Band Applications”, Micromachines, vol. 14, pp. 553, 2023.

[8] S. Tantiviwat, S.Z. Ibrahim, M.S. Razalli, “Design of Quad-Channel Diplexer and Tri-Band Bandpass Filter Based on Multiple-Mode Stub-Loaded Resonators”, Radioengineering, vol. 28, no. 1, pp. 129-135, 2019.

[9] L. Noori, A. Rezaei, “Design of a compact narrowband quad-channel diplexer for multi-channel long-range RF communication systems”, Analog Integr Circ Sig Process., vol. 94, pp. 1–8, 2018.

[10] L. Lin, Y.T. Zhao, B. Wu, C.H. Liang, “Design of Compact Quad-Channel Diplexer Using Quad-Mode Stub-Loaded Resonators”, Progress In Electromagnetics Research Letters, vol. 51, pp. 87–93, 2015.

[11] A. Zhu, H. Zhou, J. Chen, J. Li, “Compact Quad-Channel Diplexer Using Defected Stepped Impedance Resonators”, Progress In Electromagnetics Research Letters, vol. 80, 127–133, 2018.

[12] A. Rezaei, L. Noori, H. Mohammadi, “Miniaturized quad-channel microstrip diplexer with low insertion loss and wide stopband for multi-service wireless communication systems”, Wireless Networks, vol. 25, pp. 2989–2996, 2019.

[13] D. Zayniyev, D. Budimir, “Microstrip Three-Port 4-Channel Multiplexers Using Dual-Band Bandpass Filters for Wireless Applications”, 2008 IEEE Antennas and Propagation Society International Symposium, 2008.

[14] S. Khani, S. Roshani, S, Roshani, M. Fouladian, “Design and fabrication of an ultra small quadband diplexer integrated with a diplexed power amplifier for mid band 5G applications”, Scientific Reports, vol. 15, pp. 5087, 2025.

[15] J. Zhang, D. Pang, W. Wang, H. Chen, M. He, L. Ji, X. Zhang, X. Zhao, “Microstrip Quad-Channel Diplexer Using Quad-Mode Square Ring Resonators”, Microwave and Optical Technology letters, vol. 61, no. 8, pp. 2003-2007, 2019.

[16] B. Ghafari and M. Afsahi, “Design of Compact Multi-Channel Diplexer Using Defected Microstrip Structure”, Journal of Communication Engineering, vol. 8, no. 1, pp. 138-145, 2019.

[17] A. Rehman, M.U. Hassan, K. Mahmood, K.A. Awan, N.A. Wani, M.S. Anwar, “Optimized Federated Learning for Trustworthy Edge Decision-Making in IoT Consumer Electronics”, IEEE Transactions on Consumer Electronics, 2025, DOI: 10.1109/TCE.2025.3604254.

[18] K. Fizza, P.P. Jayaraman, A. Banerjee, N. Auluck, R. Ranjan, “IoT-QWatch: A Novel Framework to Support the Development of Quality-Aware Autonomic IoT Applications”, IEEE Internet of Things Journal, vol. 10, no. 20, pp. 17666-17679, 2023.

[19] S. Kumar, R. Kumar, “Design of microstrip patch antenna for IoT applications”, International Journal of Electronics and Communications (AEÜ)”, vol. 117, pp. 153-159, 2020.

[20] M.H. Alsharif, A.A. Alzahrani, “Design and implementation of a microstrip diplexer for IoT applications." Journal of Microwaves,

Optoelectronics and Electromagnetic Applications, vol. 20, no. 1, pp. 12-25, 2021.

[21] A. Mishra, &R. Kumar, "A compact microstrip bandpass filter for IoT applications", Microwave and Optical Technology Letters, vol. 63, no. 2, pp. 377-383, 2021.

[22] M.M. Rashid, M.A. Rahman, "Advanced microstrip antennas for IoT applications: Design and performance analysis", IEEE Access, vol. 10, pp:12345-12356, 2022.

[23] M.A. Khan, A. Ali, "Design of a microstrip filter for IoT applications using artificial intelligence techniques", Journal of Electrical Engineering & Technology, vol. 17, no. 4, pp. 1433-1441, 2022.

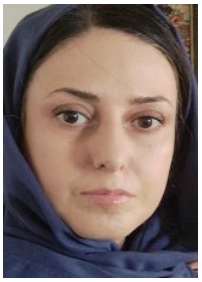

LEILA NOURI received the B.Sc. and M.Sc. degrees in electronic engineering from Razi University, Kermanshah, Iran, in 2005 and 2009, respectively, and the Ph.D. degree in electronic engineering from the Shiraz University of Technology, Iran. Now she is working in Duy Tan University as a researcher. Her research interests include microstrip devices such as filter, coupler, diplexer, triplexers, multiplexer, neural networks, wireless networks and IoT. He has published more than 70 research publications.

FARID ZUBIR (Member, IEEE) received the B.Eng. degree in electrical, majoring in telecom munication, and the M.Eng. degree in RF and microwave from the Universiti Teknologi Malaysia (UTM), in 2008 and 2010, respectively, and the Ph.D. degree from the University of Birmingham, U.K., in 2016. His Ph.D. research focused on direct integration of power amplifiers with antennas in microwave transmitters. He is currently an Assistant Professor with the Depart ment of Communication Engineering, Faculty of Electrical Engineering, UTM, and a Research Fellow with the Wireless Communication Centre, UTM. Hewasan Honorary Postdoctoral Research Fellow with The Univer sity of British Columbia (UBCO), Okanagan, Canada, from 2019 to 2021, where he conducted research on highly efficient and linear amplification power amplifier topology for wireless power systems. His research interests include RF and microwave technologies, including planar array antennas, dielectric resonator antennas (DRA), active integrated antennas (AIA), RF circuits and devices, beamforming networks, and power amplifiers.

SALAH I. YAHYA (Senior Member, IEEE) received the B.Sc. degree in electrical engineering, the M.Sc. degree in electronics and communication engineering, and the Ph.D. degree in communication and microwave engineering. He is now with the Department of Computer Technology Engineering, College of Technical Engineering, Al-Hadba University, where he is currently a Full Professor. He is a Consultant Engineer and a Senior Member of USA and AMTA-USA. He has many published research articles in high quality journals and he presented many conference papers. His research interests include antenna design, numerical RF dosimetry, MW measurement, and MW components design. He has been a regular reviewer of the Electromagnetics Academy, Cambridge, USA, PIERS Journals publications, Science and Engineering of Composite Materials Journal and International Journal of Applied Electromagnetics and Mechanics, since 2009.

MOHAMMED ABDEL HAFEZ (Senior Member, IEEE) received the B.Sc., M.Sc., and Ph.D. degrees in electrical and electronic engineering from Eastern Mediterranean University (EMU), Northern Cyprus, Turkey, in June 1992, August 1994, and November 1997, respectively. From 1992 to 1997, he was a Research Engineer with the Department of Electrical and Electronic Engineering, EMU. In 1995, he was an Instructor with the Department of Electrical Engineering, Al-Quds University. From 1997 to 1999, he was a Senior Manager with Palestine Telecommunication Company. In August 1999, he joined the Centre for Wireless Communications, University of Oulu, Oulu, Finland, as a Senior Research Scientist and the Project Manager. He is an Associate Professor of electrical and communication engineering with United Arab Emirates University, United Arab Emirates. He is also a Frequent Visiting Scientist with the Centre for Wireless Communications, University of Oulu. He has published more than 90 scientific publications. His research interests include modeling, design, and performance analysis of wireless communication systems; signal processing and system modeling; radio access; cooperative and relay networks; NOMA system; RF and microwave technologies; cognitive radio networks; microstrip devices and UWB communication.

NOORLINDAWATY MD JIZAT (Member, IEEE) received the B.E. and M.S. degrees in electrical engineering (telecommunication) from the Uni versiti Teknologi Malaysia (UTM), in 2008 and 2010, respectively, and the Ph.D. degree in elec trical engineering (telecommunication) from Mul timedia University (MMU), Malaysia, in 2024. From 2008 to 2012, she was a Quality Engi neer with Flextronics Technology Pvt. Ltd.; and a Research and Development Engineer with Pana sonic System Network Malaysia. She is currently with MMU, as a Lecturer/Researcher with the Faculty of Engineering. Her research inter ests include beamforming networks, Butler Matrix, beam steering, antenna array, self-powered solar Wi-Fi systems, and material research into antenna applications.